Arabian Journal of Geosciences (2022) 15:1482
https://doi.org/10.1007/s12517-022-10751-w

ORIGINAL PAPER

Effects of cement kiln dust on physicochemical and geomechanical properties of loess soil, Semnan Province, Iran

Ebrahim Sharifi Teshnizi[1] · Brendan C. O'Kelly[2] · Jafar Karimiazar[3] · Sayfoddin Moosazadeh[4] · Reza Arjmandzadeh[5] · Aparupa Pani[6]

Received: 1 April 2022 / Accepted: 19 August 2022

Abstract

For problematic soils, conventional (cement and lime) additives can provide the necessary improvements in geomechanical properties for various infrastructure constructions. However, these additives have a high environmental impact and they are not always cost-effective, such that potential alternative additives (e.g. obtained as industrial by-products) require investigation. This paper examines cement kiln dust (CKD), obtained as a by-product of cement clinker manufacturing, for improving the geomechanical properties of an Iranian loess soil (sandy silt). Compaction, unconfined compressive strength (UCS), direct shear (DS) strength and soaking durability tests were performed on the loess soil and its mixtures with 5–20% CKD, investigating the effect of curing period (of up to 28 days) on the mobilised strength. Observations from mineralogical and microstructural examinations are also presented in this paper. Compared to the unamended loess, the strength and elastic modulus substantially increased for increasing CKD content and curing period. Improved strength and durability (under soaking) of the soil–CKD mixtures is explained by particle aggregation (of the loess soil), inclusion of the fine CKD material and the action of calcium-derived gel (linking) products. Hence, as well as reducing the disposal problem (of the CKD by product) in the cement industry, the use of this material, as additive for soil stabilisation applications, would provide an effective and sustainable option for improving the geomechanical properties, as demonstrated for the investigated loess soil.

Keywords Cement kiln dust · Loess · Microstructural characteristics · Soil improvement

Introduction

Rapidly growing population and industrialisation are exerting tremendous pressures for infrastructure construction. Often this activity can occur in areas with inferior ground conditions from a geotechnical engineering standpoint. One such case is considered in the present paper, which examines the loess soil deposits in the semiarid to arid climate of Semnan Province, Iran. Loess is very loose to medium dense, silt soil that may be partially cemented by clay particles and salts. When dry, the loess soil is usually strong enough to support a medium-weight vehicle, but it becomes problematic when

Responsible Editor: Zeynal Abiddin Erguler

✉ Ebrahim Sharifi Teshnizi
Ebrahim.SharifiTeshnizi@mail.um.ac.ir

✉ Brendan C. O'Kelly
bokelly@tcd.ie

Jafar Karimiazar
jafarkarimiazarcivil@gmail.com

Sayfoddin Moosazadeh
s.moosazadeh@urmia.ac.ir

Reza Arjmandzadeh
r.arjmandzadeh@pnu.ac.ir

Aparupa Pani
aparupa.panifce@kiit.ac.in

1 Department of Geology, Faculty of Science, Ferdowsi University of Mashhad, Mashhad, Iran

2 Department of Civil, Structural and Environmental Engineering, Trinity College Dublin, Dublin, Ireland

3 Department of Civil Engineering, Faculty of Engineering, Seraj Higher Education Institute, Tabriz, Iran

4 Department of Mining Engineering, Faculty of Engineering, Urmia University, Urmia, Iran

5 Department of Geology, Payame Noor University, Tehran, Iran

6 School of Civil Engineering, Kalinga Institute of Industrial Technology, Bhubaneswar, Odisha, India

Published online: 03 September 2022

wet, in particular mobilising low shear strength, but also causing increased compressibility as well as other associated problems, such as a large concentration of salts. As such, loess soil deposits often do not meet the engineering quality standards required for construction of roads, foundations and other geotechnical structures (Zamani and Badv 2019; Zhang et al. 2019) and they require stabilisation utilising chemical and/or mechanical methods. Presently, cement and lime (Garzón et al. 2015, 2016; Ghadakpour et al. 2020; Jiang et al. 2020; Bahmyari et al. 2021) are widely used for soil stabilisation applications. By creating soil–cement reactions that produce primary and secondary cementitious elements, the geomechanical properties of loess soil can be improved (Nasr 2015; Zhang et al. 2017, 2019; Zamani and Badv 2019). Hydration reactions provide primary cementitious elements, consisting of hydrated $Ca(OH)_2$ and hydrated calcium silicates (C_2SHx, C_3S_2Hx). Secondary pozzolanic reactions occur between clay minerals, including silica, and alumina and hydrated lime, resulting in the formation of more calcium aluminate hydrates (C-A-H) and calcium silicate hydrates (C-S–H). Although adding cement to loess and other soils can improve their geomechanical properties, it is not always cost-effective and it can have a high environmental impact, such that there is a pressing impetus to reduce the cement consumption through effective utilisation of various industrial by-product (IBP) materials, e.g. fly ash (Elbaz et al. 2019; Zhang et al. 2019), thereby decreasing the associated greenhouse effect and environmental problems.

Industrialisation has also resulted in the production of ever-increasing quantities of IBPs, considerable resources being needed to dispose them in accordance with environmental restrictions. Consequently, there is an opportunity to explore the alternative possibility of beneficially utilising IBPs in various soil stabilisation applications. The selection of an appropriate soil additive is mostly determined by its cost and also by the qualities of the base soil, so both technical and economic studies are desirable before picking an additive for a particular project. Cement clinker manufacturing generates cement kiln dust (CKD) that must be disposed of properly. For instance, Iran produced nearly 75 million tonnes of various types of cement in 2021, with 8 million tonnes of by-product CKD mostly disposed of in landfills. CKD is gaining popularity as a construction material, including as a means of chemical stabilisation for problematic soils, thereby mitigating environmental issues associated with CKD disposal, while also providing an alternative stabilising agent to conventional cement and lime. Soil engineering properties can be improved by using CKD as a pozzolanic binder (Peethamparan and Olek 2008; Carlson et al. 2011; Albusoda and Salem 2012; Nasr 2015; Al-Homidy et al. 2017; Fakhraldin and Abdulabbas 2017; Mosa et al. 2017; Amadi and Osu 2018; Elbaz et al. 2019; Ahmad et al. 2020). Free lime (CaO), a high alkali content and a high degree of fineness (of the CKD material) have all been

Table 1 Physical and chemical properties of the investigated loess soil

	Value
Physical and index properties	
Gravel (%)	0
Sand (%)	48
Silt (%)	31
Clay (%)	21
Liquid limit (%)	35
Plastic limit (%)	30
Plasticity index (%)	5
Activity	0.24
Specific gravity of solids	2.73
USCS classification	ML
AASHTO classification	A-4
Chemical properties	
SiO_2 (%)	43.4
CaO (%)	11.9
Al_2O_3 (%)	12.5
Fe_2O_3 (%)	6.5
SO_3 (%)	5.09
MgO (%)	3.5
K_2O (%)	2.8
Na_2O (%)	0.84
TiO_2 (%)	0.55
P_2O_4 (%)	0.21
MnO (%)	0.11
Loss on ignition (%)	12.6

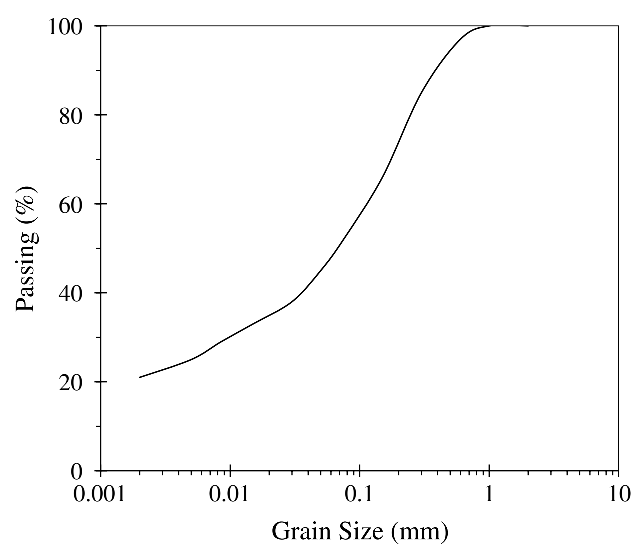

Fig. 1 Particle size distribution of the loess soil

Fig. 2 Investigated loess soil (ML) and CKD materials

shown in previous studies to make CKD a promising candidate additive for improving soil characteristics (Anwar Hossain 2011; Ahmari and Zhang 2013; Nasr 2015; Ismail and Belal 2016; Al-Homidy et al. 2017; Cui et al. 2018; Jimoh et al. 2018; Adeyanju et al. 2020; Adarmanabadi et al. 2021). Furthermore, compared to cement, CKD has the potential to penetrate fine-grained soils more efficiently, since CKD suspensions have reduced initial viscosity, meaning that they should not require high-pressure injections. The addition of 7.5%, 10%, 12.5% and 15% CKD to high plasticity clay increased the unconfined compressive strength (UCS) by about sixfold greater than that of the unamended soil (Adeyanju et al. 2020), improving its suitability as flexible pavement subgrade. However, it is worth emphasising that the soil elastic modulus and UCS improvements achieved for the CKD additive were smaller than those achieved for using cement additive (Sharma 2017; Adeyanju et al. 2020; Ogila and Eldamarawy 2022).

As described above, loess soil can be problematic for geotechnical engineering construction, the major factor being its moisture sensitivity—that is, its susceptibility to reduced bearing capacity upon exposure to moisture. Such behaviour shows that the cementing materials (e.g. gypsum, aragonite, halite, calcite), bonding the mineral grains of loess soils together, are relatively soluble in water. Research work has been published on the improvement in geotechnical properties of loess soils achieved using cement, lime and natural pozzolan (Jefferson et al. 2008; Zhang et al. 2017; Ghadakpour et al. 2020; Jiang et al. 2020; Zomorodian et al. 2020; Bahmyari et al. 2021), bio-cementation (Sun et al. 2021), nano-SiO_2 and silica fume (Kong et al. 2018; Lv et al. 2018; Sarli et al. 2020; Ghavami et al. 2021), nanoclay (montmorillonite) additive (Zomorodian et al. 2020) and root distribution (Thidar et al. 2020). However, a review of previously published research shows that the effects of CKD addition on the physicochemical and geomechanical properties of loess soils require further careful investigation.

The aim of the present investigation, therefore, is to evaluate the suitability of CKD additive in improving the undrained shear strength (and hence bearing capacity) of compacted Iranian loess soil for infrastructure construction applications. This was achieved by performing a comprehensive programme of compaction, UCS and direct shear (DS) strength testing and soaking tests (to investigate durability when immersed under water) on a loess soil sampled from Semnan Province (Iran) and of its mixtures with 5%, 10%, 15% and 20% CKD additive. The UCS and DS strength properties were investigated for 0-day, 7-day, 14-day and 28-day curing periods. Scanning electron microscopy (SEM), X-ray diffraction (XRD) and Fouriertransform infrared (FTIR) spectroscopy examinations were used to investigate differences in mineralogical and microstructural characteristics of the sampled loess soil and the 20% CKD–soil mixture.

Table 2 Physical and chemical properties of the CKD material

Chemical composition	Value (%)
SiO_2	9.82
Al_2O_3	3.64
Fe_2O_3	2.19
CaO	40.1
MgO	1.97
Na_2O	2.38
K_2O	4.67
SO_3	1.18
Insoluble residue	34.05

Experimental

Materials

The loess soil was obtained near Damghan City, Semnan Province, Iran. To prepare a homogeneous base loess soil for use in this study, ten loess samples were mixed together, and

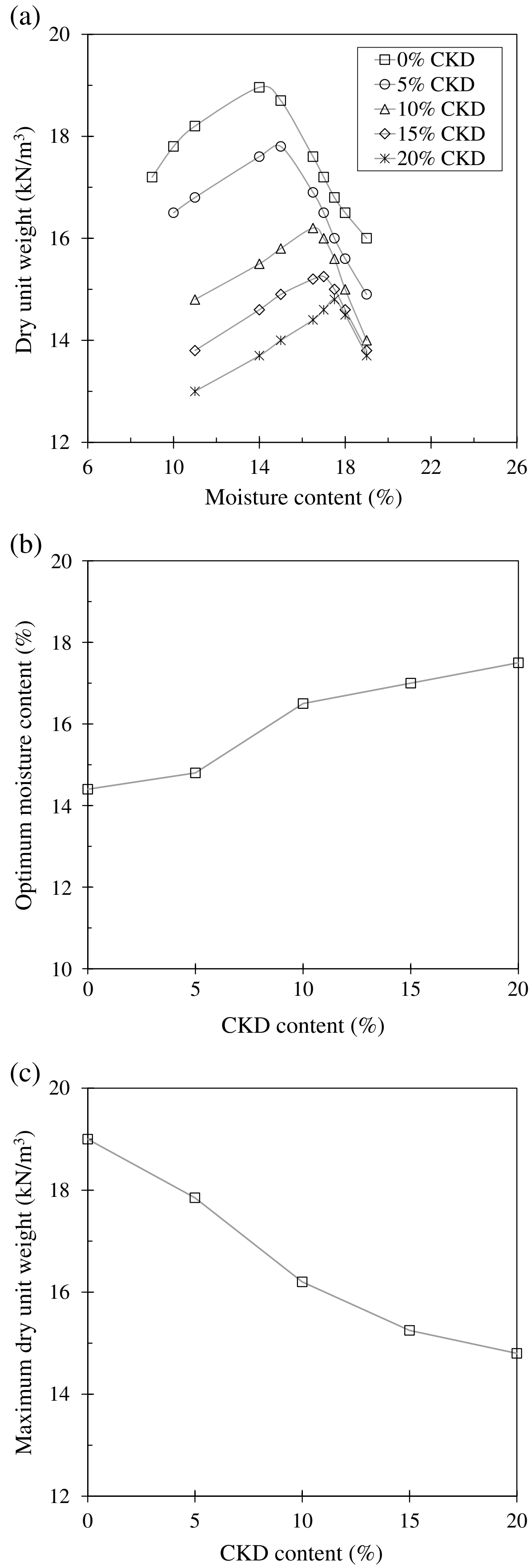

Fig. 3 Compaction results for the unamended loess soil and its mixtures with 5–20% CKD. **a** Dry unit weight against moisture content; **b** optimum moisture content against CKD content; **c** maximum dry unit weight against CKD content

then tested to determine the chemical composition, particle size distribution, Atterberg (consistency) limits and the specific gravity of the solid particles, with the results presented in Table 1 and Fig. 1. According to the Unified Soil Classification System (USCS), the soil is categorised as sandy silt (ML), whereas according to the AASHTO M145 (2008) method, the soil is categorised as A-4 material (silty soil), suggesting a "good to bad" rating subgrade.

Figure 2 shows photographs of the loess soil and CKD materials. The CKD was sourced from the Bukan cement factory in West Azerbaijan Province, Iran. The sampled material had a specific gravity of 2.95, with 83.1% by dry mass passing the #325 sieve (≤ 45 µm in particle size). Its chemical properties are listed in Table 2.

Test material preparation

The bulk loess sample was air-dried in the shade at between 25 and 30 °C, then disaggregated using a mallet, before sieving to obtain the fraction passing the ASTM #4 sieve (≤ 4.75 mm in particle size). Using subsamples of the dry soil fraction passing, various soil–CKD mixtures were prepared by thoroughly blending the soil with 5%, 10%, 15% and 20% CKD additive (dry mass basis). Test materials were then prepared with target initial water contents by adding the required amounts of water to samples of the loess soil (≤ 4.75 mm in size) and soil–CKD mixtures, while simultaneously mixing to avoid clump formation.

Methods

The geomechanical properties investigated were standard Proctor (SP) compaction and both UCS and DS strength for 0-day, 7-day, 14-day and 28-day curing periods. The compaction tests were performed according to ASTM D698 (2021). The UCS tests were conducted on 38-mm-diameter by 76-mm-long specimens according to ASTM D2166 (2016), employing an axial strain rate of 1.5%/min, with 0.2 N load sensitivity. The parameters measured were unconfined compressive strength (q_u), elastic modulus (E), axial strain at failure (ε_f) and deformability index (I_D). The DS tests were performed on 100-mm-square by 25-mm-high specimens in accordance with ASTM D3080 (2011), investigating applied normal stresses of $\sigma_v = 50$ kPa, 100 kPa and 150 kPa for determination of the cohesion (c) and friction angle (ϕ) parameters. For the strength tests, the specimens were prepared by SP compaction at optimum moisture content (OMC) to achieve the maximum

Fig. 4 UCS test results for unamended loess soil and its mixtures ▶ with 5–20% CKD, investigating specimen curing periods of **a** 7 days, **b** 14 days and **c** 28 days

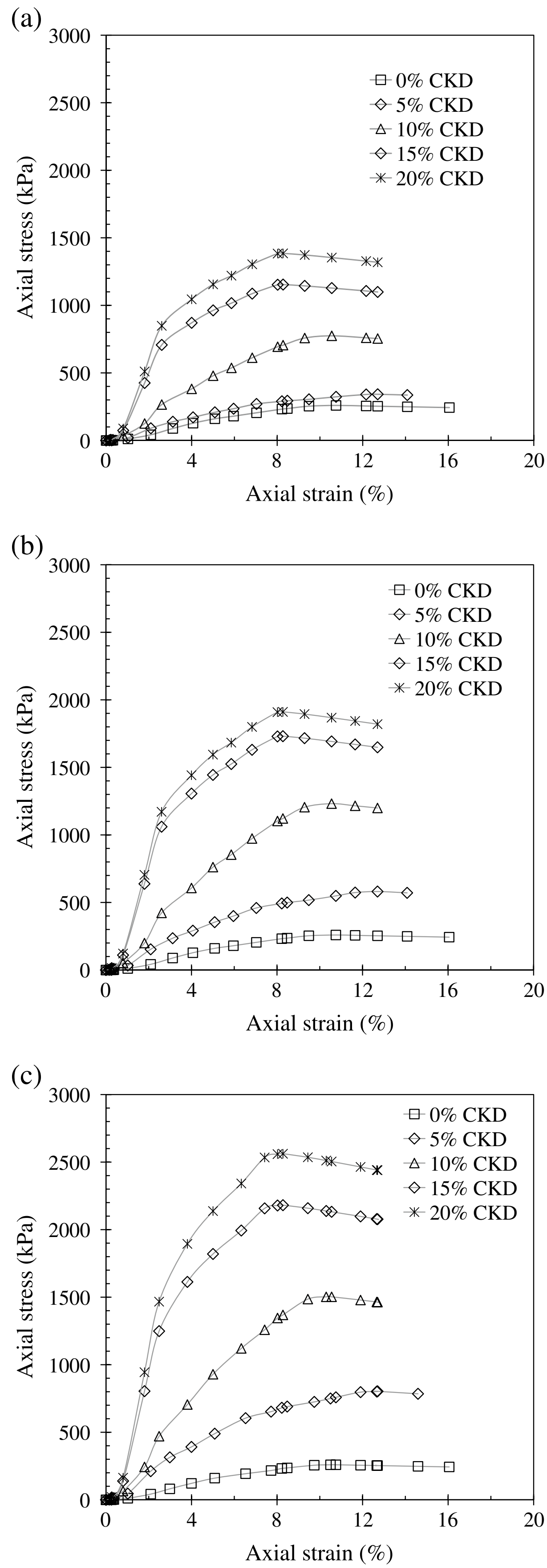

dry unit weight (MDUW). Sealed plastic bags, with a humidity level of 90%, were used to prevent any moisture loss from the prepared test specimens during their storage (in the shade) at approx. 25 °C temperature for the 7-day, 14-day and 28-day curing periods under investigation in this study. At least three replicates were tested for each testing scenario on the various soil–CKD mixtures investigated. Additionally, soaking tests were performed in accordance with ASTM D559 (2015) on compacted specimens of the unamended loess soil and its 28-day-cured mixtures with 5–20% CKD to investigate their durability when immersed under water. The test specimens, 38 mm in diameter by 76 mm long, were immersed in water, and their soaking durability/integrity was then visually monitored until such time that their failure occurred in the form of a structural disintegration/collapse.

To investigate differences in mineralogical and microstructural characteristics, SEM, XRD and FTIR spectroscopy examinations were performed on the unamended loess soil and its 28-day-cured mixture with 20% CKD. The SEM analysis was performed on representative completely dried samples using a Hitachi 4100 field emission SEM device equipped with an energy-dispersive X-ray (EDX) spectrometer. For the XRD, air dried and powdered samples, comprising particles finer than 63 μm size, were analysed with a Shimadzu XD-D1 X-ray diffractometer using the precipitation method, investigating the 2θ range of 5–100°. For the FTIR spectroscopy, a 1-mg sample mixed with 300 mg of KBr was investigated using a Shimadzu IRPrestige-21 FTIR series spectrophotometer that could measure 3600 to 700 cm^{-1} wavelengths with a resolution of 1 cm^{-1}.

Experimental results

Effect of CKD content on compaction properties

The experimental loess compaction curves, and the deduced variations in OMC (w_{opt}) and MDUW ($\gamma_{d,\,max}$) with increasing CKD content, are shown in Fig. 3. Compared to the unamended loess soil (w_{opt} = 14.4% and $\gamma_{d,\,max}$ = 18.96 kN/m^3), increasing the CKD content causes a progressive increase in OMC, whereas the MDUW progressively decreased. These outcomes follow previous research findings, with these behaviours occurring due to flocculation and cementation of the soil particles by the rapid creation of C-A-H and C-S–H gels for the CKD-amended soil, and which resulted in their reduced compactibility (Peethamparan and Olek 2008; Ahmari and Zhang 2013; Naseem et al. 2019; Mustafa et al. 2021). The OMC increase for increasing

Table 3 Summary of UCS test results

Material		Curing period (days)	UCS (kPa)	Deformability index
Loess	0% CKD (control)	0	259	1.0
Loess + CKD	5% CKD (1)	7	341	0.96
	5% CKD (2)	7	580	0.94
	5% CKD (3)	7	803	0.88
	10% CKD	7	774	0.93
	10% CKD (1)	14	1231	0.91
	10% CKD (2)	14	1502	0.86
	15% CKD (1)	14	1153	0.88
	15% CKD (2)	14	1730	0.81
	15% CKD	28	2181	0.78
	20% CKD (1)	28	1384	0.86
	20% CKD (2)	28	1910	0.80
	20% CKD (3)	28	2561	0.75

CKD addition can be attributed to the hydraulic nature of its calcium oxide component (Baghdadi et al. 1995; Miller and Azad 2000). MDUW decreases for increasing CKD content since particle aggregation occurring because of cementitious materials produces larger macro-pores within the soil–CKD mixtures (Miller and Azad 2000; Al-Homidy et al. 2017; Zhang et al. 2017; Zamani and Badv 2019).

Effect of CKD content on UCS

The UCS test results for 0-day-, 7-day-, 14-day- and 28-day-cured specimens are shown in Fig. 4. The UCS (q_u) increased

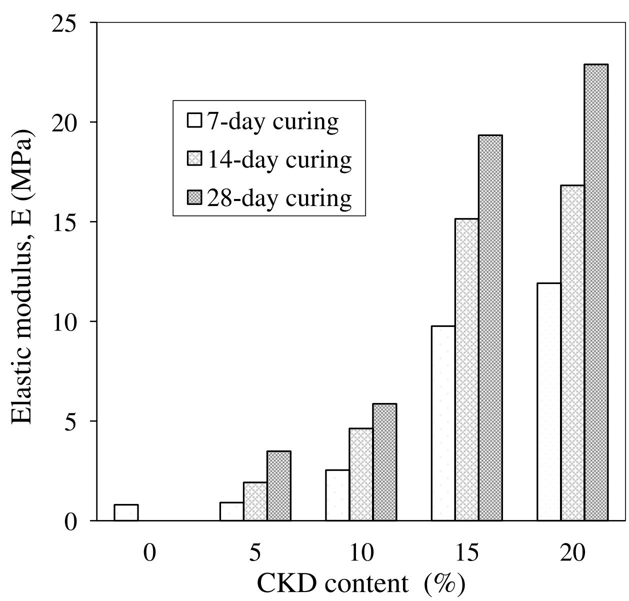

Fig. 5 Effects of CKD content and curing period on elastic modulus

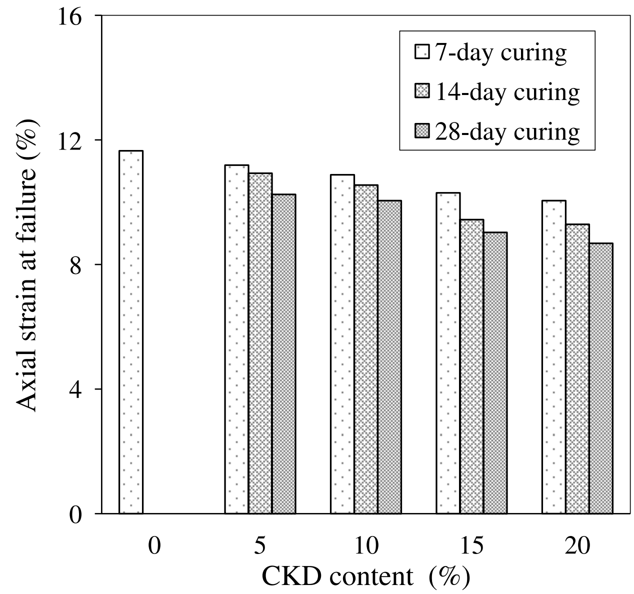

Fig. 6 Effects of CKD content and curing period on the axial strain at failure for the UCS tests

progressively for increasing CKD content and curing period, with Table 3 reporting the mobilised UCS values. For example, at 7-day curing, compared to the unamended loess soil, the mobilised UCS values for 5%, 10%, 15% and 20% CKD contents were approx. 1.3-, 3.0-, 4.5- and 5.3-fold greater, respectively. At 14-day curing, the respective UCS values were approx. 2.2-, 4.8-, 6.7- and 7.4-fold greater, while for 28-day curing, the respective UCS values were 3.1-, 5.8-, 8.4- and 9.9-fold greater.

Figure 5 shows the effect of CKD content on the elastic modulus (E) of the UCS test specimens, with its magnitude progressively increasing for increasing CKD content and curing period.

Figure 6 shows the effect of CKD content on the axial strain at failure (ε_f) (i.e. for mobilisation of peak UCS), with its magnitude decreasing marginally (i.e. the amended soil became slightly more brittle) for increasing CKD content and curing period. The test specimens' deformation behaviour was quantified in terms of the deformability index (I_D), used for explaining the brittleness/ductility behaviours of rocks and soils (Karaca and Onargan 2012). The I_D values (computed by Eq. 1) reported in Table 3 confirmed that the test specimens became slightly more brittle for increasing CKD content and curing period. Figure 7 shows the deformation behaviours at specimen failure for UCS testing of the unamended loess soil and its mixtures with 5% and 20% CKD additive. The unamended loess soil exhibited ductile behaviour (specimen bulging), with multiple cracks forming at specimen failure, whereas the CKD-stabilised soil exhibited reduced ductility, with the specimens containing 20% CKD additive being more brittle than those having 5%

CKD content. For 20% CKD content, near-vertical cracks formed at specimen failure (see Fig. 7c), indicative of a tensile specimen failure.

$$I_D = \frac{\varepsilon_{ct}}{\varepsilon_{cu}} \quad (1)$$

where ε_{ct} and ε_{cu} are the axial strains corresponding to peak UCS of the CKD-amended and unamended loess test specimens, respectively.

Effect of CKD content on DS strength parameters (c, ϕ)

Figure 8 shows the cohesion and friction angle (total stress) values deduced from the DS testing for the unamended loess soil and its mixtures with 5–20% CKD, considering curing periods of 7 days, 14 days and 28 days. As evident from Fig. 8, the cohesion and friction angle magnitudes progressively increased for increasing CKD content and curing period. That is, for 28-day curing, compared to the unamended loess soil, the cohesion values were 1.8-, 2.4-, 2.8- and 3.2-fold greater for amendment with 5%, 10%, 15% and 20% CKD contents, respectively, while the corresponding values for the friction angle were 1.11-, 1.16-, 1.25- and 1.28-fold greater, respectively.

Durability of CKD-amended specimens

Figure 9 presents the visual appearance of 28-day-cured compacted specimens of the unamended loess soil and its mixtures with 5–20% CKD after being submerged underwater for 2 days. The unamended loess soil specimen disintegrated for 6-h immersion, whereas the 5%, 10%, 15% and 20% CKD–soil mixtures were found to disintegrate for immersion periods of 12 h, 1 day, 2 days and 3 days, respectively, thereby demonstrating a substantial increase in soaking durability for increasing CKD content.

XRD and FTIR-spectroscopy analyses

The chemical properties of the unamended loess soil are reported in Table 1. XRD patterns for the unamended loess soil and its 28-day-cured mixture with 20% CKD are presented in Fig. 10. Analysis revealed the predominant minerals in the soil as quartz ($2\theta = 20.9°$, 21.9°, 26.7°, 36.6°, 42.4°, 45.9°, 50.1°, 54.9° and 59.9°), illite (26.8°), montmorillonite (24.5° and 40.7°), calcite (27.5°, 47.1° and 47.5°), hematite (56.1°) and fluorite (47.0°). As demonstrated by the emergence and alteration of peaks, the 20% CKD addition affected the soil by forming pozzolanic products because of cation exchange occurring between the soil and CKD materials. This produced a reduction in the soil clay minerals, as reflected by lower peak intensities. The stabilisation of the soil with CKD addition, and subsequent curing of the mixture, resulted in the development of C-A-H compounds (at 2θ of ~ 35.9°) — the C-A-H being created from the reaction between the alumina (Al_2O_3) in the soil and the calcium in the CKD additive. The produced C-A-H was responsible for binding of the soil particles and hence an improvement in the geomechanical properties. Additionally, in the presence of water, the calcium from CKD reacts with the alumina and silica in the soil causing the formation of C-S–H ($2\theta = 24.8°$, 29.4° and 39.4°).

Figure 11 presents the FTIR spectra for the unamended loess soil and its 28-day-cured mixture with 20% CKD, with significant differences in transmittance evident between them. For 28 days of curing, more C-S–H chains with a higher crystalline degree occur for the 20% CKD–soil mixture. The

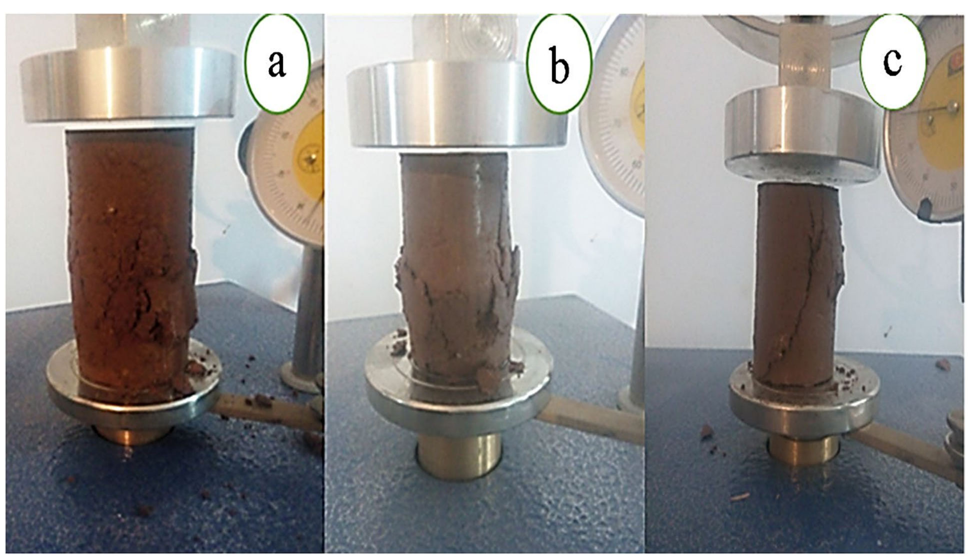

Fig. 7 Specimen failure in UCS tests. **a** Unamended loess soil; **b** 5% CKD–soil mixture; **c** 20% CKD–soil mixture

peak at 3341 cm^{-1} wavelength (which may be the stretching vibration of –O–H and bending vibration of H–O–H groups from weakly bound water molecules) was found to reduce for 20% CKD addition. Furthermore, the absorption bands ranging from 1460 to 1400 cm^{-1} (being centred at approx. 1455 cm^{-1}) were affected, with the vibrations of O–C–O being stretched, and the strong shoulder peaks at 1650 cm^{-1} and 1645 cm^{-1} are typical of O–C–O formations in the presence of 20% CKD. Similarly, Fasihnikoutalab et al. (2017) and Dang et al. (2021) reported that these bands might be

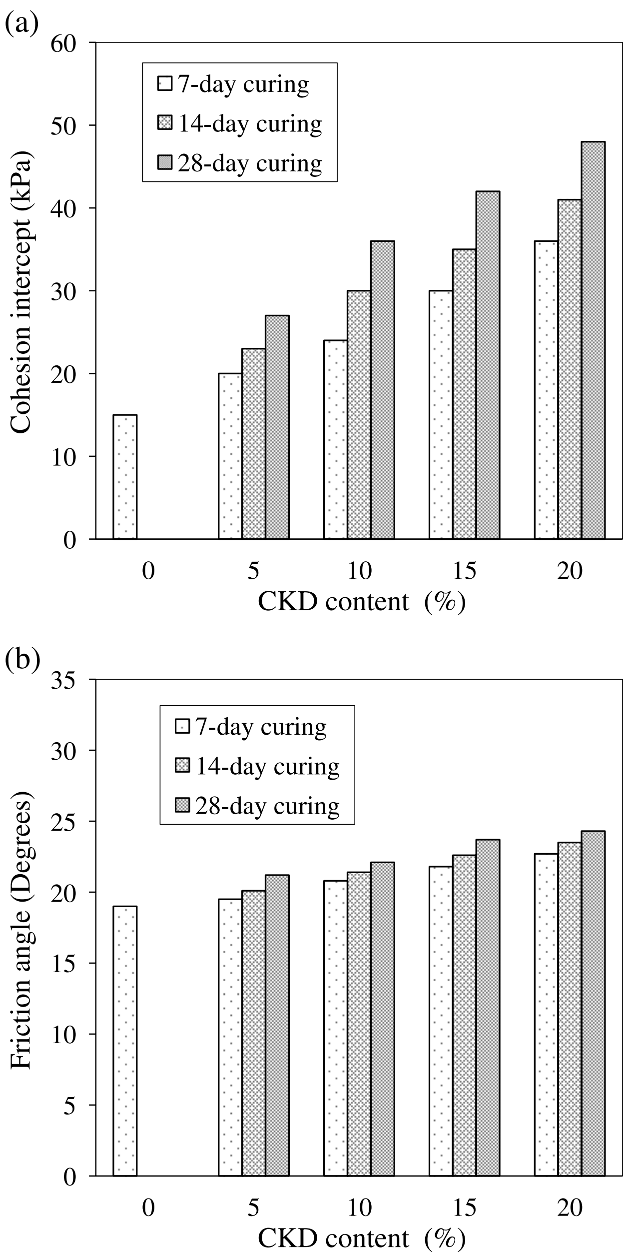

Fig. 8 Total stress direct-shear strength parameters of unamended loess soil and its mixtures with 5–20% CKD for 7-day, 14-day and 28-day curing periods. **a** Cohesion intercept; **b** friction angle

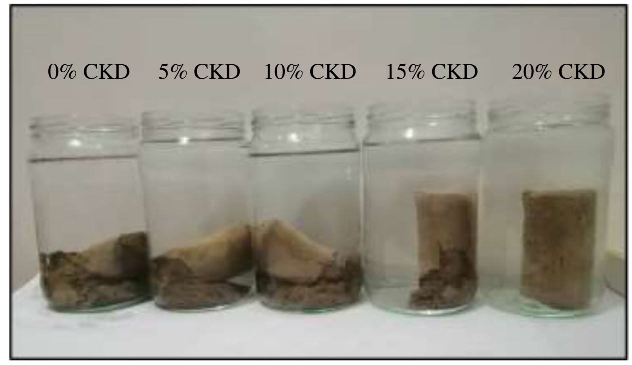

Fig. 9 Appearance of 28-day-cured compacted specimens on being submerged for 2 days in water

caused by the carbonation reaction. Figure 11 also shows that the stretching vibrations of the groups Si–O–Si and Al–O–Si, as well as the FTIR spectra of C-S–H, appeared at around 773 cm^{-1} and 680 cm^{-1}, with evidence of the Al–O–Si and Si–O–Si groups changing during the hydration process. The

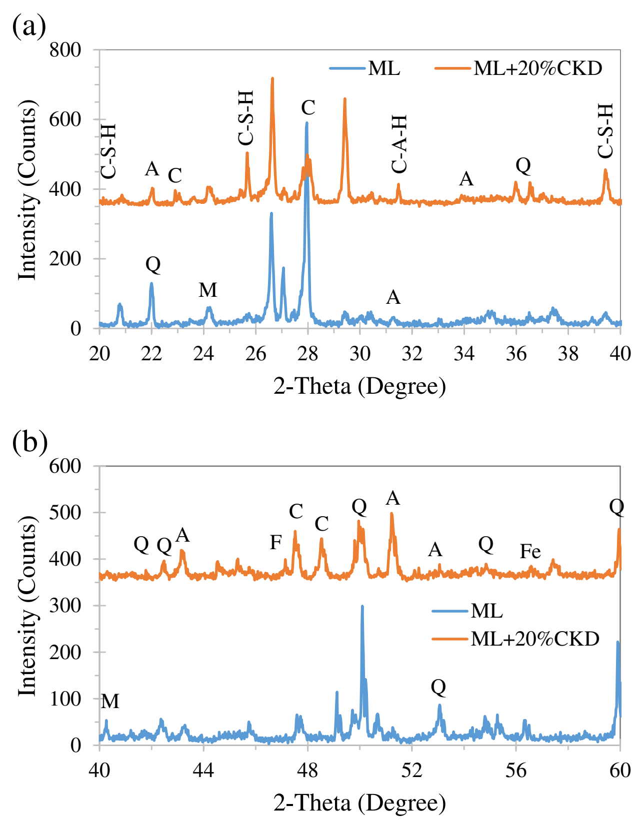

Fig. 10 XRD intensity for the unamended loess soil and its 28-day-cured mixture with 20% CKD for **a** 2θ=20–40° and **b** 2θ=40–60° (A, Al_2O_3; C, calcite ($CaCO_3$); C-A-H, calcium aluminate hydrate; C-S–H, calcium silicate hydrate; F, fluorite (CaF_2); Fe, hematite (Fe_2O_3); I, illite; M, montmorillonite; Q, quartz (SiO_2))

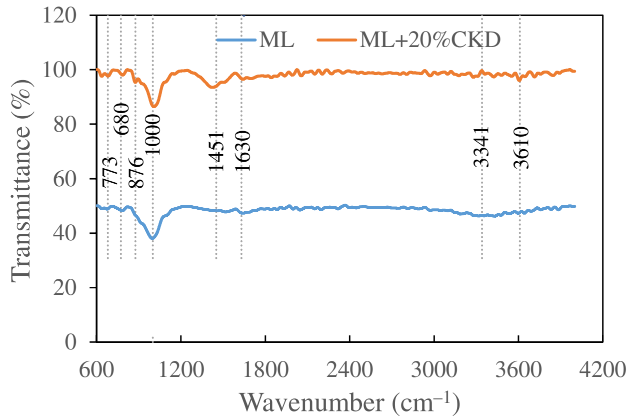

Fig. 11 FTIR spectra of the unamended loess soil and its 28-day-cured mixture with 20% CKD

dominant peaks ranging between 1100 and 950 cm^{-1}—the bands of Si–O symmetrical stretching vibration—were found to be much smaller for 20% CKD addition. Furthermore, the most increase in the strong peak for 20% CKD addition occurred at about 1000 cm^{-1}, indicative of new cementitious compounds, like C-S-H and C-A-H, being added to the microstructure. Previous studies (e.g. Salih et al. (2015) and Dang et al. (2021)) reported that when the AlO_4 tetrahedron partly replaced SiO_4, it altered how the Si–O groups occurred in the local chemical environment, such that the wavenumber of Si–O bands changes.

SEM–EDX analysis

The results of the SEM–EDX studies for the unamended loess soil and its 28-day-cured mixture with 20% CKD are shown in Figs. 12 and 13, with the latter figure presenting the spectrums of various elements present in the samples. Referring to Fig. 12a and b, the microfabric of the unamended loess soil contains a number of inter-assemblage and intra-assemblage pore spaces. Whereas for the 20% CKD–soil mixture, particle aggregation (of the loess soil), inclusion of the CKD (fine) material and action of the calcium-derived (i.e. C-A-H, C-S-H) linking products resulted in the formation of a uniform, denser fabric with reduced pore spaces (Fig. 12c and d). In other words, the increase in CKD content over the range of 5–20% investigated causes an increase in the contact area for neighbouring soil grains and improves soil particle binding. This explains the progressive improvements in the UCS and DS strength properties for increasing CKD content, as also mentioned in the papers by Miller and Azad (2000), Albusoda and Salem (2012) and Ismail and Belal (2016).

Table 4 summarises the normalised relative weight percentage (NRWP) of elements in the samples, computed as the ratio of each element measured in the sample to all elements in that sample, expressed as a percentage weight basis. Referring to Table 4, for 20% CKD addition, the intensity of the calcium (Ca) peaks decreased by 16.4% (from an NRWP of 12.2% to 10.2%), indicative

Fig. 12 SEM micrographs of **a**, **b** unamended loess soil and **c**, **d**, 28-day-cured 20% CKD–soil mixture

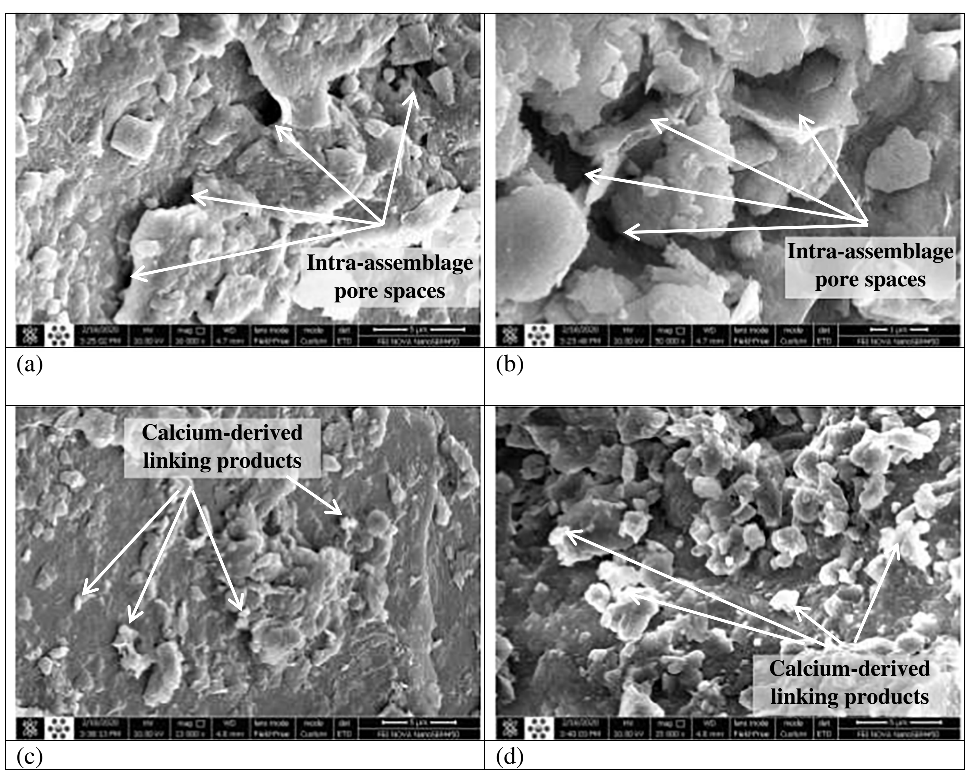

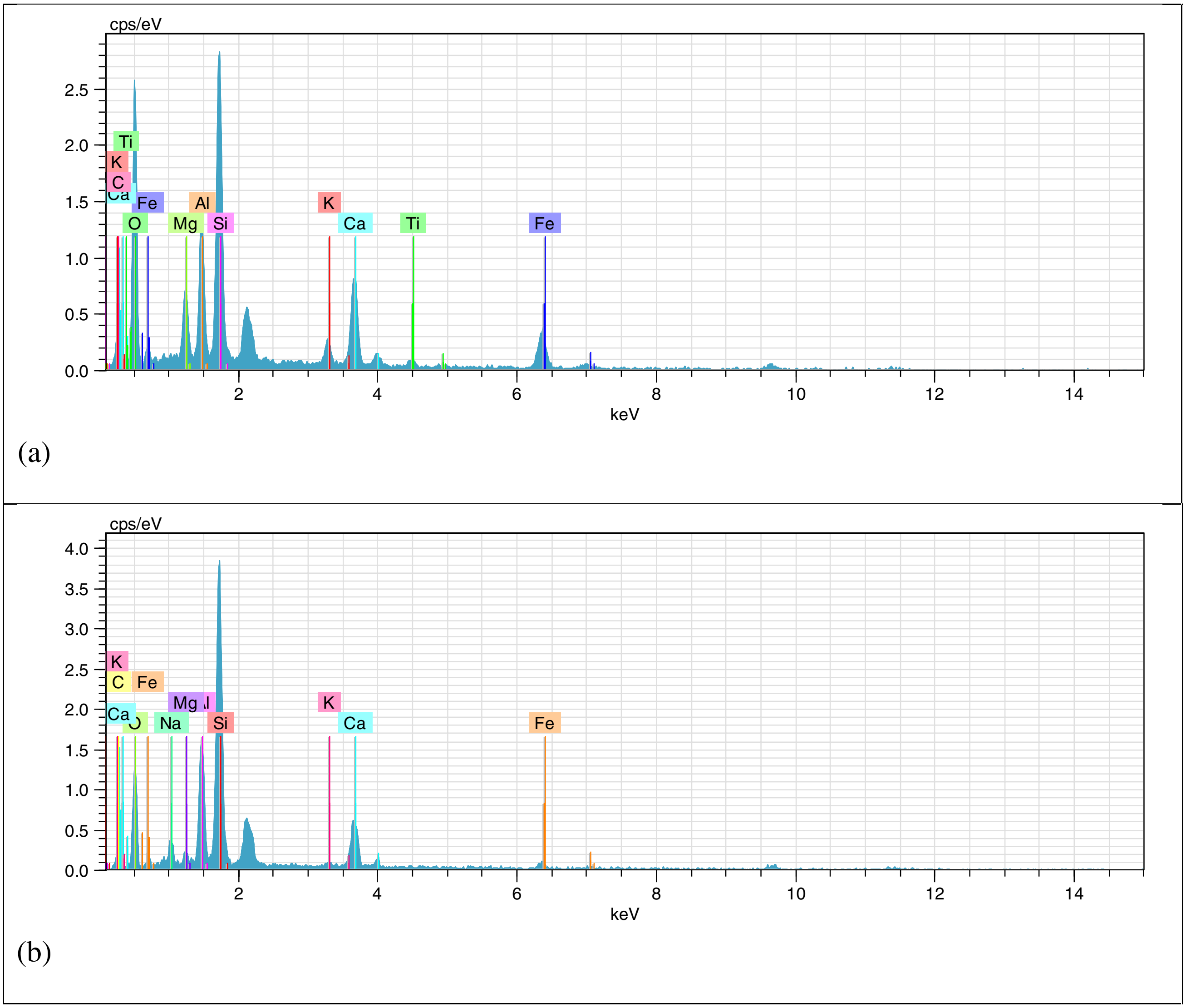

Fig. 13 Results of SEM–EDX analysis. **a** Unamended loess soil; **b** 28-day-cured 20% CKD–soil mixture. Spectrums of elements are visualised as counts/second/electron volt (cps/eV)

of the formation of C-A-H products arising from pozzolanic reactions between the fine-grained soil minerals and the CKD ions. This is consistent with observations from the SEM micrograph presented in Fig. 12. Furthermore, compared to the unamended loess soil, the intensity of the Si and Al peaks for the 20% CKD–soil mixture was significantly (112% and 81%, respectively) greater, since the CKD is rich in silica and alumina compounds.

Table 4 Normalised relative weight percentage of elements in the unamended loess soil and its 28-day-cured mixture with 20% CKD

Element	Loess soil (%)	Soil–CKD mixture (%)
Ca	12.2	10.2
Si	13.9	29.5
Al	5.9	10.7

Summary and conclusions

This study investigated the effect of 5–20% CKD addition on the geomechanical behaviour/properties of an Iranian loess soil (classified as sandy silt (ML)). The following conclusions are drawn based on the experimental results and observations from mineralogical and microstructural examinations of the unamended loess soil and the soil–CKD mixtures:

- For increasing CKD content, the OMC for compaction progressively increased, whereas the associated MDUW progressively reduced.
- Both the UCS and DS strengths, as well as the elastic modulus, all substantially increased for increasing CKD content and curing period duration. For instance, at 7-day curing, the mobilised UCS for soil mixtures with 5%, 10%, 15% and 20% CKD contents were approx. 1.3-, 3.0-, 4.5- and 5.3-fold greater, respectively, compared to the unamended loess soil, while for 28-day curing, the respective UCS mobilised were approx. 3.1-, 5.8-, 8.4- and 9.9-fold greater.
- Soaking tests indicated that, compared to the unamended, compacted loess soil, the durability of the compacted mixtures substantially improved for $\geq 15\%$ CKD addition.

The improved strength and durability (under soaking) for the soil–CKD mixtures was explained by the inclusion of the fine CKD material, particle aggregation (of the loess soil) and pozzolanic action of the C-A-H and C-S–H gel (linking) products. SEM micrographs confirmed that, compared to the unamended loess soil, CKD addition results in the formation of a uniform denser (micro)fabric with calcium-derived linking products and reduced pore spaces.

It can be concluded that, in regions where abundant CKD by-product is generated from cement production, its use as a soil additive in ground engineering applications can be an effective and sustainable option for improving geomechanical behaviour, as demonstrated for the investigated loess soil. In terms of a proper optimum CKD dosage, this will be determined by the in situ soil type, its initial physicochemical and geomechanical properties and the level of strength improvement required for a particular field application, with evidently progressively higher strength and durability achieved for greater CKD content.

Declarations

Conflict of interest The authors declare that they have no competing interests.

References

AASHTO M145 (2008) Standard specification for classification of soils and soil–aggregate mixtures for highway construction purposes. Washington, DC: AASHTO

Adarmanabadi HR, Rasti A, Razavi M (2021) The effects of cement kiln dust on the soil electrical resistivity. Am J Eng Appl Sci 14:51–63. https://doi.org/10.3844/ajeassp.2021.51.63

Adeyanju E, Okeke CA, Akinwumi I, Busari A (2020) Subgrade stabilization using rice husk ash-based geopolymer (GRHA) and cement kiln dust (CKD). Case Stud Constr Mater 13:e00388. https://doi.org/10.1016/j.cscm.2020.e00388

Ahmad S, Al-Amoudi OSB, Mustafa YMH et al (2020) Stabilization and solidification of oil-contaminated sandy soil using Portland cement and supplementary cementitious materials. J Mater Civ Eng 32:04020220. https://doi.org/10.1061/(asce)mt.1943-5533.0003169

Ahmari S, Zhang L (2013) Utilization of cement kiln dust (CKD) to enhance mine tailings-based geopolymer bricks. Constr Build Mater 40:1002–1011. https://doi.org/10.1016/j.conbuildmat.2012.11.069

Al-Homidy AA, Dahim MH, Abd El Aal AK (2017) Improvement of geotechnical properties of Sabkha soil utilizing cement kiln dust. J Rock Mech Geotech Eng 9:749–760. https://doi.org/10.1016/j.jrmge.2016.11.012

Albusoda BS, Salem LAK (2012) Stabilization of dune sand by using cement kiln dust (CKD). J Earth Sci Geotech Eng 2:131–143

Amadi AA, Osu AS (2018) Effect of curing time on strength development in black cotton soil–quarry fines composite stabilized with cement kiln dust (CKD). J King Saud Univ - Eng Sci 30:305–312. https://doi.org/10.1016/j.jksues.2016.04.001

Anwar Hossain KM (2011) Stabilized soils incorporating combinations of rice husk ash and cement kiln dust. J Mater Civ Eng 23:1320–1327. https://doi.org/10.1061/(asce)mt.1943-5533.0000310

ASTM D559 (2015) Standard test methods for wetting and drying compacted soil–cement mixtures. West Conshohocken, PA, USA: ASTM International

ASTM D698 (2021) Standard test methods for laboratory compaction characteristics of soil using standard effort (12,400 ft-lbf/ft^3 (600 kN-m/m^3)). West Conshohocken, PA, USA: ASTM International

ASTM D2166 (2016) Standard test method for unconfined compressive strength of cohesive soil. West Conshohocken, PA, USA: ASTM International

ASTM D3080 (2011) Standard test method for direct shear test of soils under consolidated drained conditions. West Conshohocken, PA, USA: ASTM International

Baghdadi ZA, Fatani MN, Sabban NA (1995) Soil modification by cement kiln dust. J Mater Civ Eng 7:218–222. https://doi.org/10.1061/(asce)0899-1561(1995)7:4(218)

Bahmyari H, Ajdari M, Vakili A, Ahmadi MH (2021) The role of the cement, lime, and natural pozzolan stabilizations on the mechanical response of a collapsible soil. Transp Infrastruct Geotechnol 8:452–472. https://doi.org/10.1007/s40515-020-00146-3

Carlson K, Sariosseiri F, Muhunthan B (2011) Engineering properties of cement kiln dust-modified soils in western Washington State. Geotech Geol Eng 29:837–844. https://doi.org/10.1007/s10706-011-9420-2

Cui SL, Wang JD, Wang XD et al (2018) Mechanical behavior and micro-structure of cement kiln dust-stabilized expensive soil. Arab J Geosci 11:521. https://doi.org/10.1007/s12517-018-3864-0

Dang LC, Khabbaz H, Ni BJ (2021) Improving engineering characteristics of expansive soils using industry waste as a sustainable application for reuse of bagasse ash. Transp Geotech 31:100637. https://doi.org/10.1016/j.trgeo.2021.100637

Elbaz AA, Aboulfotoh AM, Dohdoh AM, Wahba AM (2019) Review of beneficial uses of cement kiln dust (CKD), fly ash (FA) and their mixture. J Mater Environ Sci 10:1062–1073

Fakhraldin MK, Abdulabbas ZH (2017) Increasing shear strength parameters of sandy soil by lining CKD. Int J Curr Eng Technol 7:421–425

Fasihnikoutalab MH, Asadi A, Unluer C et al (2017) Utilization of alkali-activated olivine in soil stabilization and the effect of carbonation on unconfined compressive strength and microstructure. J Mater Civ Eng 29:06017002. https://doi.org/10.1061/(asce)mt.1943-5533.0001833

Garzón E, Cano M, O'Kelly BC, Sánchez-Soto PJ (2015) Phyllite clay-cement composites having improved engineering properties and

material applications. Appl Clay Sci 114:229–233. https://doi.org/10.1016/j.clay.2015.06.006
Garzón E, Cano M, O'Kelly BC, Sánchez-Soto PJ (2016) Effect of lime on stabilization of phyllite clays. Appl Clay Sci 123:329–334. https://doi.org/10.1016/j.clay.2016.01.042
Ghadakpour M, Choobbasti AJ, Kutanaei SS (2020) Experimental study of impact of cement treatment on the shear behavior of loess and clay. Arab J Geosci 13:184. https://doi.org/10.1007/s12517-020-5181-7
Ghavami S, Naseri H, Jahanbakhsh H, Moghadas Nejad F (2021) The impacts of nano-SiO_2 and silica fume on cement kiln dust treated soil as a sustainable cement-free stabilizer. Constr Build Mater 285:122918. https://doi.org/10.1016/j.conbuildmat.2021.122918
Ismail AIM, Belal ZL (2016) Use of cement kiln dust on the engineering modification of soil materials, Nile Delta, Egypt. Geotech Geol Eng 34:463–469. https://doi.org/10.1007/s10706-015-9957-6
Jefferson I, Evstatiev D, Karastanev D (2008) The treatment of collapsible loess soils using cement materials. In: Proceedings of GeoCongress 2008, New Orleans, Louisiana, USA (Reddy KR, Khire MV, Alshawabkeh AN (Eds)). GSP 178. ASCE, Reston, VA, USA. pp. 662–669. https://doi.org/10.1061/40971(310)82
Jiang Y, Yuan K, Li Q et al (2020) Comparison of mechanical properties of cement-stabilized loess produced using different compaction methods. Adv Mater Sci Eng 2020:4835704. https://doi.org/10.1155/2020/4835704
Jimoh IO, Amadi AA, Ogunbode EB (2018) Strength characteristics of modified black clay subgrade stabilized with cement kiln dust. Innov Infrastruct Solut 3:5–7. https://doi.org/10.1007/s41062-018-0154-3
Karaca Z, Onargan T (2012) A new approach to stone deformation: stone deformability index. Proc Inst Civ Eng – Construct Mater 165:189–195. https://doi.org/10.1680/coma.9.00031
Kong R, Zhang F, Wang G, Peng J (2018) Stabilization of loess using nano-SiO_2. Materials 11:1014. https://doi.org/10.3390/ma11061014
Lv Q, Chang C, Zhao B, Ma B (2018) Loess soil stabilization by means of SiO_2 nanoparticles. Soil Mech Found Eng 54:409–413. https://doi.org/10.1007/s11204-018-9488-2
Miller GA, Azad S (2000) Influence of soil type on stabilization with cement kiln dust. Constr Build Mater 14:89–97. https://doi.org/10.1016/S0950-0618(00)00007-6
Mosa AM, Taher AH, Al-Jaberi LA (2017) Improvement of poor subgrade soils using cement kiln dust. Case Stud Constr Mater 7:138–143. https://doi.org/10.1016/j.cscm.2017.06.005
Mustafa YMH, Al-Amoudi OSB, Ahmad S et al (2021) Utilization of Portland cement with limestone powder and cement kiln dust for stabilization/solidification of oil-contaminated marl soil. Environ Sci Pollut Res 28:3196–3216. https://doi.org/10.1007/s11356-020-10590-w
Naseem A, Mumtaz W, Fazal-e-Jalal, De Backer H (2019) Stabilization of expansive soil using tire rubber powder and cement kiln dust. Soil Mech Found Eng 56:54–58. https://doi.org/10.1007/s11204-019-09569-8
Nasr AMA (2015) Geotechnical characteristics of stabilized Sabkha soils from the Egyptian-Libyan coast. Geotech Geol Eng 33:893–911. https://doi.org/10.1007/s10706-015-9872-x
Ogila WAM, Eldamarawy ME (2022) Use of cement kiln dust for improving the geotechnical properties of collapsible soils. Indian Geotech J 52:70–85. https://doi.org/10.1007/s40098-021-00550-7
Peethamparan S, Olek J (2008) Study of the effectiveness of cement kiln dusts in stabilizing Na-montmorillonite clay. J Mater Civ Eng 20:137–146. https://doi.org/10.1061/(asce)0899-1561(2008)20:2(137)
Salih MA, Farzadnia N, Abang Ali AA, Demirboga R (2015) Development of high strength alkali activated binder using palm oil fuel ash and GGBS at ambient temperature. Constr Build Mater 93:289–300. https://doi.org/10.1016/j.conbuildmat.2015.05.119
Sarli JM, Hadadi F, Bagheri RA (2020) Stabilizing geotechnical properties of loess soil by mixing recycled polyester fiber and nano-SiO_2. Geotech Geol Eng 38:1151–1163. https://doi.org/10.1007/s10706-019-01078-7
Sharma RK (2017) Laboratory study on stabilization of clayey soil with cement kiln dust and fiber. Geotech Geol Eng 35:2291–2302. https://doi.org/10.1007/s10706-017-0245-5
Sun X, Miao L, Chen R (2021) The application of bio-cementation for improvement in collapsibility of loess. Int J Environ Sci Technol 18:2607–2618. https://doi.org/10.1007/s13762-020-02974-9
Thidar M, Gong D, Mei X et al (2020) Mulching improved soil water, root distribution and yield of maize in the Loess Plateau of Northwest China. Agric Water Manag 241:106340. https://doi.org/10.1016/j.agwat.2020.106340
Zamani M, Badv K (2019) Assessment of the geotechnical behavior of collapsible soils: a case study of the Mohammad-Abad Railway Station soil in Semnan. Geotech Geol Eng 37:2847–2860. https://doi.org/10.1007/s10706-018-00800-1
Zhang CL, Jiang GL, Su LJ, Zhou GD (2017) Effect of cement on the stabilization of loess. J Mt Sci 14:2325–2336. https://doi.org/10.1007/s11629-017-4365-4
Zhang Y, Johnson AE, White DJ (2019) Freeze-thaw performance of cement and fly ash stabilized loess. Transp Geotech 21:100279. https://doi.org/10.1016/j.trgeo.2019.100279
Zomorodian SMA, Moghispoor S, O'Kelly BC, Babaei SS (2020) Improving internal erosion resistance of silty sand using additives. Dam Reserv 30:29–41.https://doi.org/10.1680/jdare.20.00007